Title: Paired motor cortex and spinal cord epidural stimulation strengthens sensorimotor connections and improves forelimb function after cervical spinal cord injury in rats.

Abbreviated title: Paired stimulation drives motor recovery after SCI

Author names: Ajay Pal[1], HongGeun Park[1], Aditya Ramamurthy[1], Ahmet S. Asan[1], Thelma Bethea[1], Meenu Johnkutty[1], Jason B. Carmel[1,2].

Affiliations: Departments of [1]Orthopedics and [2]Neurology, Columbia University, New York, NY 10032, USA

Corresponding author email address: jason.carmel@columbia.edu

Number of pages: 48

Number of figures: 11

Number of words for abstract: 250

Number of words for introduction: 649

Number of words for discussion: 1408

Conflict of interest statement: Jason Carmel is a co-inventor of a patent for the use of softening spinal electrodes. He also has equity in Backstop Neural, which seeks to commercialize the devices for humans. The authors declare no other competing financial interests.

Acknowledgments: Research reported in this publication was supported by the National Institute of Neurological Disorders and Stroke of the National Institutes of Health under award number R01NS115470 and by the Travis Roy Foundation. We thank James McIntosh for helpful discussions about the statistical methods. We thank Tong Chun Wen for help with image acquisition. We thank Aldo Sandoval-Garcia and Walter Voit for making the spinal electrodes.

Abstract:

Associative plasticity occurs when two stimuli converge on a common neural target. We sought to use the strong convergence between motor and sensory systems in the spinal cord to restore movement after spinal cord injury (SCI). We developed a paired motor cortex and dorsal spinal cord stimulation protocol to target this interaction called spinal cord associative plasticity (SCAP). Subthreshold spinal cord stimulation strongly augments motor cortex evoked potentials at the time they are paired, but only when they arrive synchronously in the spinal cord. We tested the hypothesis that this paired stimulation effect depended on cortical descending motor and spinal cord proprioceptive afferents. Selective inactivation of either of these pathways fully abrogated the paired stimulation effect. We then found that repetitive pairing in awake rats increased spinal excitability for hours after pairing ended. To apply this protocol as therapy, we optimized the parameters to promote strong and long-lasting effects. This effect was just as strong in rats with cervical SCI as in un-injured rats, demonstrating that spared connections after SCI are sufficient to support this plasticity. When 30 minutes of paired stimulation was done over 10 days, the effect of pairing was sustained for weeks. In addition, H-reflex modulation improved, showing decreased hyperreflexia that also persisted for weeks. Importantly, repetitive paired stimulation supported enhanced recovery of forelimb dexterity in rats after SCI with no augmentation of injury-induced neuropathic pain. We conclude that SCAP strengthens sensory-motor connections within the spinal cord, resulting in decreased hyperreflexia and improved forelimb function after SCI.

Significance Statement:

Despite evidence that electrical stimulation of spared nervous system connections can facilitate recovery after SCI, strongly overlapping sensory and motor connections in the spinal cord have not been targeted for therapy. Here we demonstrate a robust paired stimulation paradigm that depends on corticofugal and

proprioceptive afferent convergence in the spinal cord. The paradigm, termed SCAP for spinal cord associative plasticity, produced large-scale physiological changes in a preclinical model of cervical SCI. Importantly, SCAP caused lasting improvements in dexterity and decreased hyperreflexia in rats with SCI. Thus, we have determined the neural circuits that drive SCAP and have preclinical evidence for its efficacy to restore function after incomplete cervical SCI, the most common SCI in people.

Introduction:

Paired electrical stimulation employs similar mechanisms to change neural connections as those used to learn associations. For nervous system recovery, associative plasticity has been used to improve arm and hand function. Many have targeted the motor system to strengthen direct connections between motor cortex and spinal motoneurons. Two-site electrical stimulation is timed to converge in the spinal cord and promote lasting changes in motor evoked potentials (MEPs) and improved grip strength and finger control (Bunday and Perez, 2012; Bunday et al., 2018; Jo and Perez, 2020). Intraspinal stimulation in monkeys has been timed with cortical activity so endogenous brain activity and exogenous spinal cord stimulation converge (Nishimura et al., 2013a, 2013b). Repetitive pairing induced a small but significant increase in MEPs.

In contrast to efforts targeting the motor system, the most common paired stimulation protocol in people targets motor and sensory integration in the cortex. Paired associative stimulation repetitively pairs median nerve stimulation with motor cortex stimulation timed to increase cortical excitability in healthy people (Stefan et al., 2000) and improve arm and hand function after injury (Suppa et al., 2017; Ling et al., 2020). Using a similar logic but targeting the spinal cord, epidural stimulation has been used to drive activation of spinal afferents that can be timed to converge with descending motor activation. This strategy helped to restore walking after SCI, but only when spinal stimulation was timed to coincide with motor

cortex signals arriving in the spinal cord (Capogrosso et al., 2016). We use paired stimulation to strengthen residual connections after cervical spinal cord injury, the most common type (NSCISC, 2020). For people with cervical SCI, recovery of arm and hand function is the highest priority (Anderson, 2004).

Since integration of descending motor control with spinal sensory feedback is critical for skilled movement, we target these interactions by pairing motor cortex and cervical spinal cord stimulation to mediate spinal cord associative plasticity (SCAP; (Mishra et al., 2017). The convergence of subthreshold spinal cord electrical stimulation with a descending cortical volley robustly augments the cortical MEP. When this pairing is performed repeatedly, there is an increase in excitability that lasts for at least an hour. This plasticity requires paired stimulation delivered at the proper time, but the exact neural circuits that mediate the sensorimotor interactions are not known. In addition, this process has been demonstrated in anesthetized rats and it was unknown how SCAP might change in awake, behaving animals. Perhaps most importantly, the protocol was previously tested in uninjured rats, and it was not known whether the sparse connections that remain intact after SCI were sufficient to support SCAP and recovery of function.

We hypothesized that repetitive pairing of motor cortex and spinal cord stimulation would augment spinal excitability and improve function in rats with SCI through spinal sensory and descending motor convergence. To test how SCAP works in awake and freely-moving rats, we created spinal stimulating electrodes that can be inserted into the thin epidural space over the cervical spinal cord, are supple enough to conform to the spinal cord, and move with the neck (Garcia-Sandoval et al., 2018). These were used to measure and modulate the nervous system, which can be challenging in awake animals due to variability in MEPs (Gerasimenko et al., 2006). We optimized the SCAP protocol to counter this variability and to improve efficacy.

Finally, we addressed the necessary and sufficient neural circuits for SCAP. To determine necessity, we selectively inactivated descending corticospinal circuits using a 2-virus system. We also inactivated spinal afferents, including specific inactivation of proprioceptive afferents, using transgenic rats. To understand whether the circuits preserved by cervical SCI are sufficient for SCAP, we tested the protocol in rats with moderate C4 contusion. We then examined the efficacy of SCAP delivered over 10 days for changes in physiology, modulation of reflexes, and recovery of dexterity. Together, these experiments were designed to improve our understanding of SCAP mechanisms and to test its efficacy for recovery of dexterity after SCI.

Materials and Methods:

Experimental overview: The experiments were designed to test the mechanisms of SCAP and its efficacy on physiology and function in rats with SCI. We first tested the timing of motor cortex and spinal cord stimulation with the hypothesis that timing to converge in the spinal cord would produce the largest changes in physiology. We tested the necessity of corticospinal and segmental afferent connections for SCAP by selectively inactivating each with a chemogenetic tool. To optimize the SCAP protocol, we varied the parameters of frequency, number, and pattern of stimuli. We tested this optimized 30-minute protocol against the original 5-minute protocol. To determine whether the circuits mediating SCAP we sufficiently spared, we tested the effects of SCAP in rats with C4 spinal cord contusion. Finally, we performed a randomized, blinded preclinical trial of 10 days of SCAP versus sham stimulation to determine the effects on physiology and paw function.

Animals: Thirty-eight adult female Sprague-Dawley rats (Charles River, bodyweight of 275 +/- 25 grams) were used in this study: 22 rats were uninjured and 16 rats received spinal contusion. Of the rats with spinal contusion, 5 died immediately after SCI. To test the proper timing of brain and spinal cord

stimulation, a group of 4 healthy rats were tested on the immediate effect of adding subthreshold spinal cord stimulation to suprathreshold cortical stimulation (Fig. 1). To understand which neural circuits mediate these effects, 8 rats had inactivation of neural circuits. Three rats were used for CST inactivation (Fig. 2), two for sensory afferent inactivation (Fig. 3A-C), and 3 PV-Cre rats were used for proprioceptor inactivation experiments (Fig. 3D-F). To test the effects of repetitive brain and spinal cord stimulation (SCAP), 10 healthy rats were used for the development and testing of SCAP (Figs. 4,5&6). To determine whether the neural circuits spared by SCI could support SCAP, 11 rats were subjected to a moderate cervical (C4) contusion. Two injured rats were initially used to test the short-term efficacy of SCAP. To test the long-term efficacy of SCAP to restore physiology and function, a group of 9 rats were randomized to real (n=5) or sham (n=4) SCAP repeated over 10 days.

Surgery and Care: For all surgical procedures, rats were anesthetized via intraperitoneal injection of a mixture of ketamine (90 mg/kg) and xylazine (10 mg/kg body weight). Local application of bupivacaine (0.25- 0.5%, 0.1-0.2mL) was done before making skin incision and buprenorphine (0.05 mg/kg body weight, subcutaneous) was administered before and after the survival surgery and also after H-reflex testing to alleviate pain. Anesthesia levels were monitored by respiration and heart rate and responses to foot pinch. Animals were placed on heating pads (PhysioSuite, Kent Scientific Corporation, Northwest CT, USA) to maintain a body temperature of 37.5°C as measured continuously by a rectal probe (PhysioSuite). The animals were housed in individual cages with free access to food and water on a 12/12-hour light/dark cycle. All experimental procedures were in full compliance with the approved Institutional Animal Care and Use Committee Protocol of Columbia University.

Cortical electrodes, EMG wire, and spinal stimulator implantation: In a single procedure, motor cortex screw electrodes and EMG wires were placed and the head connectors brought to the common head cap. Rats were anesthetized and head-fixed in a stereotaxic frame (David Kopf Instruments, Tujunga, CA,

USA). The skull was exposed and placement holes made using a Jobber Drill (number 60, P1 Technologies, Roanoke, VA, USA) without disturbing the dura mater. Stainless steel screw electrodes (1.19 mm diameter with a flat tip; Plastics One, Torrington, CT, USA) were implanted over the forelimb area of the motor cortex in one hemisphere at two locations as described in our previous work ((Mishra et al., 2017)). The screw electrodes were attached in advance to a head connector (Plastics One) that was secured with skull screws and dental acrylic. For electromyogram (EMG) recordings, we inserted supple stainless steel braided wire (diameter = 0.014mm; #AS 634, Cooner Wire Co., Chatsworth, CA, USA) electrodes into the biceps muscle (for MEPs) and adductor digiti minimi (#AS 631, for H-reflex). For the biceps, the other end was tunneled subcutaneously and attached in advance to a head connector, mounted on the skull, and also secured with skull screws and dental acrylic (Lang Dental Manufacturing Co., Inc., Wheeling, IL, USA).

One week after a cortical and EMG electrode implant, the rats went through another surgery to implant spinal stimulation electrodes, as described previously (Garcia-Sandoval et al., 2018). Briefly, the head was fixed and the cervical spine. The T1 spinous process was clamped to stabilize the spine. The C4 spinal cord was exposed by laminectomy. Array electrodes were placed in the dorsal epidural space in the midline of the spinal cord over C5-C6. Muscles and skin were sutured in layers. The array head connector was mounted on the skull and also secured with skull screws and dental acrylic.

MEP measurements (Fig. 1): All the MEP measurements were done in awake behaving rats in their home cages. Before the start of testing, electrodes were connected and the animal was left in the cage for 10-15 minutes to get habituated. We stimulated the motor cortex and measured MEPs from contralateral biceps muscle. Both motor cortices were stimulated independently and contralateral EMGs acquired from the biceps. A similar primary motor cortex and spinal cord stimulation paradigm were used as described by Mishra et al., 2017. Briefly, a train of three biphasic square wave pulses (each pulse of 0.2 ms for each

polarity; interstimulus interval of 3 ms; Fig. 1A) was used for motor cortex stimulation. Multichannel EMG signals were acquired before and after the repetitive stimulation at 5,000Hz sampling rate, with a CED (CED Micro 1401, Cambridge Electronic Design Ltd, Cambridge, UK) data acquisition system and a recording software (Signal 5.08, CED Ltd). The signals were amplified at a gain of x1000 and bandpass filtered 1–1000Hz with an integrated AC differential amplifier system (A-M Systems, Model 1700, Sequim,WA, USA). Motor cortex and spinal stimulation were performed using an isolated pulse stimulator (A-M Systems, Model 2100). MEPs were extracted, processed, and quantified using customized Motometrics analysis (Ratnadurai Giridharan et al., 2019).

For the motor cortex stimulation we first measured the cortical threshold, defined as the stimulation intensity needed to evoke a short latency MEP in > 50% of trials, by stimulating cortex at increasing intensities. We then measured the MEP at 110% of the cortical threshold, which we call cortical MEPs. The same method was then used to determine the spinal threshold and to measure MEPs at 110% of spinal threshold, which we call spinal MEPs. For the paired stimulation, we stimulated the motor cortex at 110% of cortical threshold and the spinal cord was stimulated with 90% spinal threshold intensity. To quantify MEPs, the electromyograms (EMGs) were rectified and then averaged across 20 trials. The area-under-the-curve (AUC) was calculated for MEPs and % change from baseline was quantified. To determine the most effective latency, we stimulated the spinal cord at various time intervals from 30 ms before motor cortex stimulation to 30 ms after motor cortex stimulation. Latencies were tested in a randomized sequence, with a minimum of 2 minutes between each test.

CST inactivation (Fig. 2): The corticospinal tract was selectively inactivated using a Designer Receptor Exclusively Activated by Designer Drug (DREADD), during paired stimulation. To target the corticospinal tract selectively, a Cre-dependent adeno-associated virus (AAV) encoding the DREADD was injected into the motor cortex and another encoding Cre-recombinase was injected into the cervical

spinal cord. Thus, only doubly infected neurons express the DREADD, which can be inactivated by the administration of its ligand, clozapine-N-oxide (Park and Carmel, 2016). Through a craniotomy, twelve injections of 200nl of AAV1-hSyn-DIO-hM4D(Gi)-mCherry {2 x 10^{12} vg/ml, pAAV-hSyn-DIO-hM4D(Gi)-mCherry was a gift from Bryan Roth (Addgene viral prep # 44362-AAV1 ; http://n2t.net/addgene:44362 ; RRID:Addgene_44362) (Krashes et al., 2011)} were made 1.5 mm from the pial surface into the forelimb area of the left motor cortex at the following forelimb motor cortex coordinates (Brus-Ramer et al., 2009): AP 0.5 ML 1.5; AP 0.5, ML 2.5; AP 0.5, ML 3.5, AP 1.5, ML 1.5; AP 1.5, ML 2.5; AP1.5, ML 3.5; AP 2.5, ML 1.5; AP 2.5, ML 2.5; AP 2.5, ML 3.5; AP 3.5, ML 2.0, AP 3.5, ML 3.0; AP 4.5, ML2.5. AAV5/retro-pmSyn1-EBFP-Cre (5.5 x 10^{12} vg/ml, AAV pmSyn1-EBFP-Cre was a gift from Hongkui Zeng; Addgene viral prep # 51507-AAV5; http://n2t.net/addgene:51507 ; RRID:Addgene_51507; (Madisen et al., 2015) was injected into the right side of the cervical spinal cord. 11 injections of 200 nl of AAV were made in C5 and C6, 0.8 mm lateral from the midline at the depth of 1.2 mm from the surface of the spinal cord, with 0.6 mm intervals between injections.

One week after AAV injections, animals were trained on the vermicelli handling task (Allred et al., 2008; Wen et al., 2018). After reaching a stable baseline performance, the number of forepaw manipulations was measured before, during, and after inactivation. The number of adjustments of each forepaw was counted while the animal was eating uncooked pasta before and at 30, 60, and 120 minutes after intraperitoneal injection of 2.4 mg/kg body weight of clozapine N-oxide (CNO). One week after the behavioral test, we tested the effects of inactivation on the immediate effects of paired brain and spinal cord stimulation. Under deep anesthesia a cranial window was created to expose the forelimb motor cortex, and silver ball electrodes were placed over two locations: 1.0 mm anterior, and 2.0 mm lateral; and 3.0 mm anterior and 4.0 mm lateral to bregma. After that we exposed the C4-C6 vertebrae, and laminectomy was done at C5-C6 level to expose dorsal surface of spinal cord and a pair of silver ball

electrodes were placed epidurally on the midline of C5-C6 cervical spinal cord. A pair of EMG wires were inserted in the biceps muscle bilaterally to record EMG. Systemic administration of CNO typically causes maximum inactivation of DREADD expressing neurons within 30 minutes, and CNO typically washes out within two hours (Wahl et al., 2014). This allows testing of physiology and behavior before, during, and after reversible inactivation of specific neural circuits. The MEP of each biceps was tested by independent stimulation of the contralateral motor cortex. At each timepoint, the effects of subthreshold spinal cord stimulation were compared with brain only stimulation. Measurements were taken every 10 minutes for 2 hours.

Afferent inactivation (Fig. 3): The necessity of afferents for the immediate effects of paired stimulation was tested using two inactivation strategies. For the first strategy, large diameter dorsal root ganglion (DRG) neurons were inactivated. Large DRG neurons mediate touch, proprioception, and muscle length/tension (Giuffrida and Rustioni, 1992). The specificity of large-diameter DRG neurons was provided by the tropism of the AAV5 (Vulchanova et al., 2010). One microliter of AAV5-hSyn-hM4D(Gi)-mCherry (2 x 10^{13} vg/ml, pAAV-hSyn-hM4D(Gi)-mCherry was a gift from Bryan Roth (Addgene viral prep # 50475-AAV5; http://n2t.net/addgene:50475 ; RRID:Addgene_50475) was injected into each DRG at C5, C6, and C7 on one side of the spinal cord after partial laminectomy. At the time of virus injection, stainless steel screw electrodes were placed over each motor cortex, spinal array on the epidural surfaces of C5-C6 cervical spinal cord, and EMG wires in the biceps muscle bilaterally. Similar to CST inactivation, four to five weeks after the virus injection, large-diameter afferents were inactivated by an intraperitoneal injection of 2.4 mg/kg body weight of CNO and MEPs measured over 2 hours. For the second strategy, we targeted the proprioceptive afferents for inactivation, since these mediate the effects of spinal cord stimulation (Takeoka et al., 2014; Asboth et al., 2018). We used a genetic strategy to target DRG neurons that express parvalbumin, which are proprioceptors (Ichikawa et al., 1994; Walters

et al., 2019). In transgenic rats that express Cre recombinase under the control of parvalbumin promoter PV-Cre rats (LE-Tg(Pvalb-iCre)2Ottc, Optogenetics and Transgenic Technology Core, NIDA, MD, USA obtained via Rat Research Resource Centre RRRC#773; the genotype was confirmed prior to virus injections by PCR using the primers, Pvalb forward: 5'-CCG TTC AGC TTG AAG GTG TC-3', iCre R12: 5'-CAC AGT CAG CAG GTT GGA GA-3') we injected a Cre-dependent DREADD (AAV5-hSyn-DIO-hM4D(Gi)-mCherry (2 x 10^{13} vg/ml, pAAV-hSyn-DIO-hM4D(Gi)-mCherry was a gift from Bryan Roth; Addgene viral prep # 44362-AAV5; http://n2t.net/addgene:44362 ; RRID:Addgene_44362; (Krashes et al., 2011) into the C5, C6, and C7 DRGs as described above. Inactivation with CNO and physiology measurement were also identical. In these rats cortical and EMG electrodes were implanted one week before DRG injections, and the spinal array was implanted just after the injection using the methods described above.

SCAP Optimization (Fig. 4): In order to maximize the efficacy of the SCAP protocol (Mishra et al., 2017), we varied four parameters in order to produce the largest physiological responses: frequency, number of stimuli, number of trains, and time between trains. In two rats implanted with cortical and spinal electrodes, we first varied frequency by testing 10 stimuli delivered at 5Hz, 2 Hz, 1Hz, 0.5Hz and 0.2Hz (Fig 4A). We tested whether repeated stimuli suppressed the resulting MEP. For the other parameters, we examined the short term SCAP effects with the average percent increase in cortical MEPs and spinal excitability over the 120 minutes after the SCAP protocol (Fig. 5). Spinal excitability was used since this was less variable than spinal MEPs, and out of concern that eliciting spinal MEPs might induce plasticity. In addition, we intended to keep the total stimulation period to 30 minutes, a period that could be used for stimulation in people. For these trials, we used 5 Hz pairing and varied the number of stimuli by comparing 150, 75 & 38 pulses. For subsequent trials we used 150 stimuli, which we term a train, and varied the number of trains, either 10 or 20 (Fig. 4B). For subsequent trials we used 20 trains and varied

the time between trains, either 1 or 5 minutes. The optimized 30-minute SCAP protocol is shown in Fig. 5B2. A train of 150 stimuli at 5Hz frequency (30 seconds) is followed by a 60-second gap. The train and gap is then repeated 20 times, delivering 3000 stimuli pairs in 30 minutes.

SCAP (Figs. 5 & 6): We tested brain and spinal cord responses at baseline and then after the period of repetitive pairing (Fig. 5), as we did in Mishra et al., 2017 but in awake rats with implanted electrodes. This differs from the immediate effects of stimulation (Fig. 1). Before modulation, we measured the stimulation threshold for the motor cortex to produce a MEP in 50% of trials and also the spinal threshold. We then stimulated with 110% of threshold to determine cortical and spinal MEPs, using the area under the curve. At baseline, cortical and spinal MEPs, as well as cortical and spinal thresholds were measured singly and independently (Fig. 5A). For repetitive pairing (Fig. 5B), motor cortex stimulation was performed at 110 % of the threshold for evoking a cortical MEP followed 10 ms later by spinal cord stimulation performed at 90% of the threshold for generating a spinal MEP. After repetitive pairing (Fig. 5C), the same measures taken at baseline were taken immediately after pairing and every 20 min thereafter up to 120 min. We quantified excitability as 1/threshold and expressed as % change from baseline.

Rat cervical contusion SCI: The C4 spinal cord contusion surgery was performed as previously described (Yang et al., 2019). Briefly, the C3 to C5 vertebrae were exposed by skin incision and muscle separation on the midline. Laminectomy of C4 was performed, taking care to ensure the dura remained intact. Following laminectomy, the rat was placed on the Infinite Horizon (IH) impactor stabilization platform (IH-0400, Precision Systems and Instrumentation, LLC), and the C3 and C5 spinous processes were clamped. A fine adjustment was made to the vertebral clamps to ensure that the exposed C4 spinal cord surface was level. The moderate contusion injury was made with a 3.5 mm impactor tip raised to three complete turns ~2 mm from the dorsal surface and was dropped with a preset 200 kdynes force on to the spinal cord with no dwell time. The force curve of the impactor was saved so that the rats in the

Stim and Control groups could be compared. After injury, the rat was removed from the platform and the spinal electrode array was implanted as described above.

Rats received intense care after SCI. This included placing their cage on a heating pad for 12 h, administering buprenorphine (4 doses in total, 0.05 mg/kg) every 8–12 h, and Baytril (5 mg/kg, Norbrook, Henry Schein, Melville, NY) daily for 5 days. For nutrition, Ringer's Lactate solution (10 ml, subcutaneous) was administered daily for 5–10 days and Diet boost Gel (ClearH2O, Portland, ME) was placed within reach until rats regained the ability to reach the food and water dispensers. Body weight, food and water intake was monitored daily. Bladders were palpated every 12 hours; none of the rats showed bladder dysfunction.

SCAP in SCI rats (Figs. 6, & 8): We designed a preclinical efficacy trial, as shown in Fig. 7. Ten days of an optimized SCAP protocol was delivered in the subacute period, 10 days after injury (Yang et al., 2019); (Carmel et al., 2010). The daily stimulation duration (30 minutes) and number of sessions (10) were designed to be clinically viable. The primary outcome measure was the dexterity (IBB) score, and secondary outcomes included changes in MEPs, H-reflex modulation (a measure of hyperreflexia), and a pain measure (RGS). The study was powered based on the effect size we observe of a different neuromodulation strategy ((Yang et al., 2019). The a priori power analysis suggested needing 8 rats in each group to achieve a power of 0.8. However, the physiological effects of SCAP were more robust than the previous paradigm, suggesting a stronger behavioral effect. The post-hoc power with a total of 9 rats was 0.63 using the same parameters as the initial power calculation.

Randomization and blinding procedures: Rats were pseudorandomized into real (Stim) and sham (Control) groups with each cohort of up to 6 rats having rats assigned to each group. Rats were randomized immediately after SCI surgery, and experiments were carried out with blinded measures. The experimenter

who randomized rats into different groups and performed paired stimulation treatment, but was not involved in behavior tasks training, testing or scoring process or in histology. Experimenters who performed behavior training, testing, and scoring and histology did not participate in randomization, electrophysiology testing, or paired stimulation. Control rats were connected to the stimulator, but no stimulation was delivered. Since all rats had both cortical and spinal electrodes implanted, there was no way to distinguish by appearance whether rats received stimulation.

H-reflex testing (Fig. 9): To track hyperreflexia, we measured the H-reflex at baseline, one week after SCI, just after 10 days of stimulation and every two weeks post-stimulation (Fig. 7). The M-wave is evoked by the excitation of motor axons. The H-reflex is the electrophysiological equivalent of the spinal stretch reflex; Ia proprioceptive afferents synapse on and activate motor neurons in the spinal cord (Fig. 9A). Rats were lightly anesthetized with 60 mg/kg ketamine. A pair of braided wire electrodes were inserted across the medial plantar side of the wrist to stimulate the ulnar nerve (via a constant current isolated pulse stimulator, stimulus width 100µs, A-M Systems). Two recording electrodes were inserted into the abductor digiti minimi to record electromyograms. The threshold was determined as the lowest stimulation intensity that elicited an H-wave response in at least 75% of the recordings (Tan et al., 2012). First, we tested responses to increasing stimulus intensities up to 2X threshold, which activates low threshold afferent fibers. Next, we tested the frequency-dependent depression of the H-wave (Tan et al., 2012); (Kathe et al., 2016; Mekhael et al., 2019). This is also commonly referred to as post-activation depression or as rate-dependent depression. We stimulated every 10 s with paired stimuli at inter-stimulus intervals from 10 s to 0.01 s. The H-wave area under the curve (AUC) of the test stimulus was normalized to the H-wave AUC of the conditioning stimulus. 25 paired stimuli per frequency were averaged and plotted as a frequency-depression curve (Fig. 9C & D).

Behavior testing (Fig. 10): Food Manipulation Task (IBB): To assess the rats ability to manipulate, we used the Irvine, Beatties, and Bresnahan scale (Irvine et al., 2010; Irvine et al., 2014), as we have before (Yang et al., 2019). All rats were placed in a clear plastic cylinder on top of a rotating carousel so that they could be rotated in the direction of the video camera. The rats were habituated to the testing environment for 10 days, 15 minute per day. For testing, rats were videoed while eating both donut-shaped (Froot Loops, Kellogg's NA Co.) and sphere-shaped (Reese's Puffs, General Mills Sales Inc.) cereal. Experimenters blinded to treatment recorded the rats eating the cereals before SCI and weekly from 4 to 7 weeks after SCI. Analysis of the recorded session was done offline by a blinded observer. The scores for the two different kinds of cereal and the two forepaws were averaged. An schematics showing characteristic features of rat forelimbs during cereal manipulation task is presented in fig.10A. Images of a representative stimulation rat were generated from frames of live videos with the image tracing tool of Adobe Illustrator software.

Rat Grimmace Scale (RGS): This scale is used to quantify pain using the rats facial characteristics (Sotocinal et al., 2011), the way that is commonly used to assess pain in people. All rats were kept on a rotating carousel as in the case of the food manipulation task, and the facial features were recorded with a camera by a blinded experimenter at the times shown in Fig. 10. The facial features were analyzed offline by a blinded scorer.

SCI histology (Fig. 11): To determine the severity of SCI, we compared the parameter (at the time of SCI) and severity of injury between those with and without therapeutic stimulation. One week later, rats were deeply anesthetized and perfused, first with ~400 ml 0.1M phosphate-buffered saline (PBS) containing 5,000 UPS units/ml of heparin, and then with 600 ml 4% paraformaldehyde. Spinal cord (C1-T2) were dissected and post-fixed in 4% paraformaldehyde for 48 h. The tissue was then transferred to 30% sucrose at 4°C until it was cut in the coronal section at 40μm thickness on a cryostat. Tissue

sections from C3 to C5 were processed for lesion reconstruction. Spinal cord sections were collected serially and directly onto slides to preserve tissue integrity. The tissue sections dried overnight and were coverslipped the next day. The outline of the lesion, grey matter, and white matter were traced using darkfield microscopy and Neurolucida software (MBF Bioscience, Williston, Vermont, USA). The lesion was reconstructed by a blinded experimenter using the 3D visualization tool. The Cavalieri Estimator probe in Stereo-investigator (MBF Bioscience) was used to determine lesion and total tissue area for sections rostral, caudal, and at the epicenter of the lesion. The spared tissue area was computed by subtracting the lesion tissue area from the total tissue area. To compare the extent of injury in the two groups, spared tissue area data was quantified every 3 slices for the whole injury length (Yang et al., 2019).

Statistical Analyses:

All of the comparisons between stimulation conditions were done with paired t-tests with Bonferroni correction. To determine the latency for paired stimulation (Fig. 1), we compared MEPs for pairing at different latencies to the baseline (only motor cortex stimulation at 110% of threshold). For the inactivation experiments (Figs. 2 & 3), the immediate effects of the pairing on the targeted side at baseline was compared to the different times after CNO injection. For SCAP (Figs. 4&6), we used only descriptive statistics as percentage change in MEP. Independent cortex and spinal MEPs were compared to each time after SCAP. For the preclinical randomized trial, the Stim and Control groups were compared by an independent t-test with Bonferroni correction. The immediate effects of pairing was compared between the groups at several time points (Fig. 8). H-reflex modulation was compared only at the shortest (0.01s) inter-stimulus-interval (Fig. 9). The dexterity and pain scores were compared at the end of the trial (Fig. 10; day 50). To compare the injuries (Fig. 11), the peak force delivered to induce SCI (mean± sem force at the time of impact was presented) and percentage spared tissue area at the epicenter between the groups

was compared independent t-test. All the statistical analysis was performed with SPSS (SPSS Statistics for Windows, version 27; IBM Corp., Armonk, NY, USA). We tested the normality of the data using the Shapiro-Wilk test. All data are expressed as Mean ± SEM.

Results:

The overall hypothesis was that repetitive pairing of motor cortex and spinal cord would augment spinal excitability and improve function in rats with SCI through spinal sensory and descending motor convergence in the spinal cord. This hypothesis was tested in steps. First, we tested convergence in the spinal cord by altering the timing for SCAP. Second, to determine whether the CST and proprioceptors were necessary for SCAP, we selectively inactivated each. Third, we optimized the SCAP protocol. Fourth, we tested whether the connections preserved by cervical SCI were sufficient to enable SCAP by performing modulation in rats with SCI. Finally, we tested whether 10 days of repetitive SCAP improved physiology and behavior after SCI.

Spinal stimulation augments cortical responses when properly timed

We hypothesized that stimulating the spinal cord at the time that descending motor potentials arrive would most strongly augment cortical MEPs (Fig. 1A). In awake rats with implanted electrodes, the motor cortex was stimulated at 110% of the MEP threshold (suprathreshold; Fig. 1B), and the cervical spinal cord was stimulated at 90% of threshold (subthreshold). Spinal cord stimulation augmented cortical MEPs at multiple time points (Fig. 1C) with a strong peak when the spinal cord was stimulated 10ms after the motor cortex (183% ± 31%, df=6, Cohen's d=4.82, $p < 0.0001$). We paired the motor cortex and cervical spinal stimulation at various latencies (Fig. 1C). To understand why the peak occurred at this time, we recorded from the spinal epidural electrodes after cortex stimulation. After the initiation of a train of 3 stimuli in the motor cortex, the cord dorsum potential arrived at 9.17± 0.55ms

(Mean ± SEM, n=3), very similar to the peak around 10ms. There were also smaller increases in MEPs when the spinal cord was stimulated 20ms before cortex (22% ± 6%, df=6, Cohen's d=2.37, $p = 0.022$) and when the sites were stimulated at the same time (0ms; 28% ± 6%, df= 6, Cohen's d= 2.97, $p = 0.012$), similar in timing to what we had observed in anesthetized rats (Mishra et al., 2017) but with a larger effect.

Effects of paired stimulation are mediated by corticospinal and proprioceptive afferents

To test the hypothesis that descending corticospinal circuits and large-diameter afferents are necessary for the effects of pairing, we selectively inactivated each with a chemogenetic tool. We hypothesized that inactivation of either of these circuits would eliminate the effect of paired stimulation.

To test the necessity of corticospinal neurons for the paired stimulation effect, they were selectively inactivated using a 2-virus system (Fig. 2A). A virus encoding an inhibitory DREADD that requires Cre-recombinase was injected into the motor cortex, and a retrograde virus encoding Cre-recombinase was injected into the spinal cord. In rats with these injections, layer 5 neurons in the motor cortex were selectively and robustly labeled (Fig. 2B). To test whether inactivation produces functional inactivation, we observed the effects on paw use while the rats ate uncooked pasta, a test of dexterity (Allred et al., 2008). The number of manipulations with each paw was measured at baseline and then at several times after administration of clozapine-N-oxide, the ligand for the inhibitory DREADD. At the time of maximum inactivation {30 min; (Wahl et al., 2014)} the number of manipulations the rat made while eating uncooked pasta with the paw targeted for inactivation diminished by 60% (Fig. 2C). The number of manipulations partially recovered by 120 minutes, as the CNO washed out. Manipulations in the non-targeted paw were not highly affected. These results indicate that selective corticospinal neuron inactivation diminishes paw use on the inactivated side.

We then tested whether this inactivation abrogated the effects of paired stimulation (Fig. 2D). At baseline (BL), subthreshold spinal cord stimulation delivered 10ms after suprathreshold motor cortex stimulation strongly augmented biceps MEPs (>150%). Administration of CNO caused the MEP augmentation to be diminished compared to baseline, and at 30 minutes, spinal cord stimulation had no augmenting effect on motor cortex MEPs on the inactivated side. The effects of pairing recovered by the end of the 120-minute testing period. On the non-inactivated side, there was a less pronounced and more delayed effect of inactivation. Thus, corticospinal neurons are necessary for the effects of paired stimulation.

To determine if paired stimulation also depends on spinal afferents, we inactivated dorsal root ganglia (DRG) neurons using two methods. First, we targeted large-diameter neurons; an AAV5 encoding an inactivating DREADD was injected into DRGs of C5 and C6 on one side (Figure 3A). Cells infected with the virus (Figure 3B) measured 68±18μm in diameter, similar to neurons that mediate touch, proprioception, and muscle length/tension (Giuffrida and Rustioni, 1992). Before inactivation, the pairing of brain and spinal cord stimulation caused a large augmentation of the biceps MEP (>100%; Figure 3C, red) compared to baseline. Thirty minutes after CNO injection, the paired stimulation effect was abolished (-1.5% ±10.5%, df= 4, Chone's d= 2.34, p= 0.013) and largely returned by 120 minutes. There was no significant effect on the non-targeted side.

For the second approach, we selectively targeted the proprioceptors. A Cre-dependent DREADD was injected into the DRGs of transgenic rats expressing Cre under control of parvalbumin, which is expressed selectively by proprioceptors (Fig. 3E; (Giuffrida and Rustioni, 1992)). Inactivation caused a large-scale, but incomplete, abrogation of paired stimulation (Fig. 3F, green). The loss of paired stimulation effect with inactivation of proprioceptors was less than non-selective (red) inactivation, thus, inactivation of large-diameter DRG neurons, and largely proprioceptors, abrogated the effects of paired

stimulation. These results show that large-diameter sensory afferents inputs are necessary for the effects of SCAP.

SCAP protocol optimization

We optimized SCAP to increase MEPs after a stimulation period of 30 minutes, a period that is tolerable for clinical neuromodulation (Fitzgerald, 2020). We tested 4 parameters: frequency of pairing (Fig. 4A), pulse number (length of train), time between trains and number of bursts/trains (Fig. 4 B). We tested five frequencies (Fig. 4A) to determine if each pair of stimuli would cause inhibition or augmentation of subsequent stimuli. The 5Hz and 0.2Hz frequencies produced little change between stimuli, and we selected 5Hz to minimize the total duration of stimulation. We also observed that 1Hz was strongly inhibitory. Using the 5Hz frequency, we tested other parameters as shown in Fig. 4C. For the length of the train, 150 stimuli was better than the others tested. For the time interval between two bursts, we observed that the 5-minute interval was slightly better than 1 minute, but we selected 1 minute to minimize the total duration of stimulation. Finally, we tested the total number of repetitions of bursts/trains. We observed that 20 trains of stimulation had a more durable effect than 10 trains (data not shown) with a similar overall magnitude. This resulted in the paradigm pictured in Figure 5.

SCAP causes lasting changes in cortical and spinal cord excitability in uninjured rats and rats with SCI

We tested the hypothesis that SCAP would produce lasting increases in spinal excitability, where the descending motor and segmental afferent connections converge. Specifically, we predicted that repeated pairing would cause lasting increases in MEPs and excitability for both motor cortex and spinal cord stimulation. We hypothesized that 5 min SCAP would produce larger responses than we reported in our previous work with anesthetized rats (Mishra et al., 2017). As shown in the blue lines of Figs. 6A & 6B,

the 5 minute protocol nearly doubled the size of the MEPs and increased excitability. These changes were of a similar magnitude but much longer duration than we previously reported; anesthetized rats had no increase in MEPs after 60 minutes.

We further hypothesized that the 30-minute SCAP protocol would produce stronger effects than the original 5-minute SCAP protocol (Fig. 5). The physiological effects of the optimized 30-minute paradigm were more robust; the peak response was higher (black & grey lines, Figs. 6A & B), and the effects longer-lasting. MEPs were approximately doubled, and although the effects declined over the testing period, they were still ~50% larger than baseline at 120 minutes. Thus, SCAP in awake rats produces large increases in MEPs and excitability that last for hours.

We also tested the effects of SCAP in rats with SCI. Following the 5 minute SCAP protocol, changes in MEPs and excitability in rats with SCI were slightly less robust and more transient than in uninjured rats. This indicates that the physiological effects of the optimized 30-minute SCAP paradigm are more robust than our published 5-minute SCAP paradigm in both intact and injured animals.

We then calculated the average percent change over 120 minutes in order to compare the efficacy of SCAP paradigms to control conditions (motor cortex alone, spinal cord alone, or paired with spinal cord stimulation after a 100 ms delay). None of these control conditions drove an increase in MEP magnitude (Fig. 6E). Immediately after 30 minutes of paired stimulation, rats with SCI and uninjured rats had augmented cortical and spinal MEPs. In rats with SCI, the effect of SCAP was similar between cortical and spinal MEPs. Finally, the similar magnitude and duration of effects in intact and injured rats suggests that circuits spared by SCI are sufficient to mediate pairing effects.

SCAP causes lasting increases in excitability and improves reflex modulation over weeks

To determine whether SCAP might be used to restore sensorimotor function after SCI, we performed a preclinical efficacy trial (Fig. 7). We hypothesized that SCAP delivered daily over 10 days in rats with SCI (SCI+stimulation group) would strengthen sensorimotor connections and improve function more than rats without stimulation (SCI-no stim. control group). To probe the strength of connections, we measured the efficacy of paired stimulation by its immediate effect (Fig. 8). This measure is very stable over time, since the augmentation is always compared to a baseline MEP of cortical stimulation alone. In both groups of rats with SCI, the immediate effect of pairing was large at 11 days after SCI (~150%), before the start of stimulation (Fig. 8). In the stimulation group, cortical MEP augmentation increased over the 10-day period to 246 ± 36%, while the control group did not change (161%+/-22%). The difference between groups was maintained at 50 days after SCI (Stim = 275%+/-25% vs Control = 166%+/-12%, df = 7, Cohen's d= 2.74, p=0.005). This indicates that repetitive pairing over a 10-day period creates a durable change in physiology.

We hypothesized that repetitive stimulation would help restore spinal reflex modulation. We tested H-reflex modulation before and after SCI. The ulnar nerve at the wrist was stimulated and monosynaptic H-reflex was recorded from abductor digiti minimi (Fig. 9A). Then H-reflexes were elicited at different interstimulus intervals to modulate responses (Fig. 9B). Before injury in both rats with SCAP (Fig. 9C) and controls (Fig. 9D), shorter intervals between H-reflexes caused the second one to be diminished (blue lines). SCI diminished the rate-dependent decrease in the H-reflex (top lines), consistent with hyperreflexia. Ten days of SCAP largely restored rate-dependent depression of the H-reflex (9C; bright red lines). In contrast, control rats had little to no recovery of H-reflex modulation (9D; gray lines). This effect was still persistent at 50 days after SCI (30% more modulation compared to the control group; df= 7, Cohen's d=4.64, p=0.0001). Thus, SCAP decreased hyperreflexia after SCI.

SCAP improved forelimb dexterity without changing affective pain

Finally, we tested the behavioral effects of 10 days of paired stimulation. To test dexterity, rats were trained and tested by a blinded observer on the Irvine, Beatties, and Bresnahan (IBB) test, a scale that measures paw function while eating pieces of cereal (Irvine et al., 2010). Before SCI, all rats performed at the top of the 9-point scale (Fig. 10A). Twenty-eight days after SCI, the rats in each group showed equivalent and severe impairment (stimulation= 2.55; control= 2.79), with difficulty holding and manipulating the cereal. By 50 days after injury, the last time tested, control rats scored 3.45 ± 0.74, and rats with stimulation scored 5.36 ± 0.22, demonstrating better grasp and support of the cereal (Fig. 10B).

To test the effects of stimulation on pain, we used the rat grimace scale (RGS), which uses facial features to rate severity on a two-point scale (Sotocinal et al., 2011). All rats showed pain after SCI (Fig. 10C), despite being given analgesics, which diminished by 3 weeks and stayed low. There was no difference in pain scores between the groups at the end of the trial (50 days; df =7, Cohen's d= 0.126, p=0.51). Thus, SCAP improved dexterity and did not produce pain.

No difference in SCI and tissue sparing between stimulation and control groups

We quantified the peak force rats received during C4 spinal contusion and the spared tissue preserved at the injury site at the end of the trial. The peak force that rats received is shown in Fig. 11A. There was no significant difference between the stimulation group (210 ± 2 kilodynes, n=5; df= 7, Cohen's d= 0.446, p= 0.17) and the control group (214 ± 6 kilodynes, n= 4). We also compared the amount of tissue spared by the injury throughout the area of the whole length of the lesioned spinal cord. Rats in both the control and the stimulation groups exhibit the similar pattern of injury. Representative spinal cord sections showing the lesion epicenter and rostral and caudal to epicentre are shown in fig 11B. We quantified the area of spared tissue area throughout the lesion and expressed it as a percentage of the cross sectional area of the perimeter of the tissue (Fig. 11C). There was no significant difference between the control (2.78±

0.39 mm^2, mean ±SEM) and the stimulation group (2.25± 0.47 mm^2, independent t-test, df= 7, Cohen's d=0.333, p=0.629). We concluded that the injury rats received are similar between stimulation and control groups.

Discussion:

Our main hypothesis proved true: repetitive pairing of motor cortex and spinal cord augmented spinal excitability and improved function in rats with SCI through spinal sensory and descending motor convergence. This conclusion was built stepwise through three main experiments. First, both CST and spinal proprioceptors are necessary for the augmenting effects of paired stimulation, since inactivating each abrogated the immediate effects of pairing timed to converge in the spinal cord. Second, the connections preserved by cervical SCI were sufficient to enable SCAP, since the effects of paired stimulation were as robust in rats with SCI as uninjured controls. Third, SCAP improved physiology and behavior after SCI: excitability was increased after a single session, and with a durable effect when repeatedly administered, while hyperreflexia was diminished. Forepaw manipulations were improved and pain was not altered in rats receiving repeated SCAP. Below, we discuss the knowledge gained, the remaining gaps, and the possibility of translation of this approach.

SCAP depends on sensorimotor convergence in the spinal cord

Our model of SCAP as the convergence of descending sensory and segmental proprioceptors at the level of the spinal cord is supported by 3 lines of evidence. First, there is striking concordance between the time that motor potentials arrive in the spinal cord (9.17± 0.55ms) and the optimal latency (10ms) for pairing for the immediate effects. Second, this immediate effect depends on the CST and proprioceptors, as demonstrated by abrogation of the effect with selective inactivation of each of these pathways (Figs. 2 &

3). Finally, pairing of motor cortex and spinal cord at a latency that has no immediate effect (100ms) also produces no plasticity when applied repetitively (Fig. 6F).

Knowing the site of convergence and the pathways that mediate the effects of paired stimulation may enable more accurate targeting and sets up future comparisons with other neuromodulation strategies. Changes in the placement of electrodes and stimulation parameters may allow more effective and selective stimulation of the motor and sensory connections that converge to produce SCAP. Comparisons to other paradigms might include manipulations of the descending (upper) motor system and segmental (lower) motor system (Taylor and Martin, 2009; Nishimura et al., 2013a; Harel and Carmel, 2016; Chandrasekaran et al., 2020; Jo and Perez, 2020) or sensory and motor connections timed to arrive in the brain. Given that these approaches target different systems or sites of convergence, these approaches might be combined to harness the effects of each.

SCAP effective in rats with moderate cervical SCI

SCAP was at least as effective in rats with C4 SCI as uninjured rats, indicating that sparse descending motor circuits mediate the plasticity effect, along with the intact sensory system below injury. The C4 contusion injury obliterates the gray matter and leaves just a thin rim of white matter, similar to human injury (Bunge et al., 1993; Kakulas and Kaelan, 2015). Interestingly, we observed sparing of <1% of the CST in rats with this injury (Yang et al., 2019). This suggests that other descending motor pathways may be involved, as they are in recovery after human SCI (Baker and Perez, 2017). Targeting the reticulospinal tract, which is slightly better preserved by experimental SCI in rats, results in improvement of motor function, both in rodents (Asboth et al., 2018; Moritz, 2018) and in humans (Bunday et al., 2018; Sangari et al., 2019).

The reliance of paired stimulation on the CST in uninjured rats and likely independence in injured rats can be explained by two alternative hypotheses. First, there may be tract switching: the CST might mediate the effects of pairing in uninjured rats and the cortico-reticulo-spinal pathway in rats with SCI (Raineteau et al., 2001; Starkey et al., 2012; Wahl et al., 2014). Against this idea is that 10ms is the optimal time for pairing in both groups; if tract switching occurred, it is likely that the latency would also shift. Alternatively, the cortico-reticulo-spinal pathway might mediate the descending motor component in both uninjured and SCI rats (Baker and Perez, 2017; Asboth et al., 2018; Engmann et al., 2020). Although the 2-virus inactivation strategy is highly selective for the CST, this might also inactivate cortico-reticular connections; pyramidal neurons in the motor cortex send projections to many subcortical targets, including the medullary reticular formation and the spinal cord (Bastmeyer and O'Leary, 1996; Gu et al., 2019) So inactivation of the CST may also inactivate cortical connections to the reticular formation. We intend to test the idea directly by inactivating the reticulospinal tract in rats with and without SCI. As we better define the pathways that mediate the effects of paired stimulation, we may get closer to a longstanding goal of neuromodulation, which is to deliver stimulation based on the pattern of spared connections.

There is a striking concordance of physiological changes induced by SCAP at the cortical and spinal cord levels. This is likely explained by changes in responses in the spinal cord, possibly in the common target of descending motor and segmental afferent connections. These results contribute to our working model that convergent inputs to spinal neurons cause the synapses or the cellular targets themselves to undergo lasting change. Synchrony of input is critical, since paired stimulation with an inappropriate time difference between motor cortex and spinal cord stimulation was ineffective in producing plasticity.

Long-lasting improvements in physiology and behavior with 10 days of stimulation

Paired stimulation produces effects on 3 time scales: immediate, hours, and weeks. The immediate effects (Fig. 1) do not represent plasticity; they operate only at the time that subthreshold spinal stimulation augments cortical MEPs. For paired stimulation to promote plasticity, it must be repeated. Our optimized repetitive stimulation protocol produces robust augmentation that was still 50% greater than baseline at 2 hours after 30 minutes of pairing. Thus, some effects are short lived, on the order of hours. However, when SCAP was delivered for 10 days, we detected changes that lasted the entire study period (at least 4 weeks from the end of the stimulation period). This includes stronger MEPs with paired stimulation (Fig. 8) and decreased hyperreflexia (Fig. 9). These represent two critical functions of the sensorimotor system, to drive voluntary movement and to modulate segmental reflexes (Porter and Lemon, 1995; Wolpaw, 2018).

We have built our paradigm by optimizing at each time scale before moving on to the next. The best latency for immediate effects was used for SCAP. The SCAP variables that produced the largest and longest-lasting effects were then used for the 10-day application. This process produced a large effect, but the assumption that optimal conditions for effects on one timescale are also optimal for another has not been tested. This may depend on the biological processes mediating each of these effects and whether they are conserved. In addition, like many neuromodulation approaches, we have not optimized the most durable effects, including duration, frequency and timing of repetitive SCAP, among many other parameters. Testing these parameters in rats would provide an optimized preclinical paradigm for translation.

The functional recovery was limited in two important ways. First, the final time point tested was 7 weeks after injury, a time that paw function was still improving in the rats with stimulation. Thus, the full extent of the improvement is not known. We also do not know the durability of the effects beyond this 7-week period. In addition, there were a relatively low number of rats in this portion of the study,

owing, in part, to the high mortality rate (31%) after SCI. Randomization happened after SCI. The a priori power analysis predicted a power of 0.63, based on our recent study of a different neuromodulation paradigm (Yang et al., 2019). Insofar as the large physiological effects of SCAP might translate into more robust behavioral results, the power might be higher with this intervention. The study showed significant improvement in dexterity using the a priori primary outcome measure.

Translation

This study provides important considerations for the application of paired stimulation to enhance sensorimotor function in people. The interactions between descending motor pathways and large-diameter afferents is largely conserved between rats and humans, but the direct connections between motor cortex and spinal motoneurons in humans may alter these interactions. In addition, the scale of the two species is very different, and it will be important to determine the proper timing of paired stimulation in people. Finally, the differences in the location of tracts within the spinal cord and the pattern of injury to the spinal cord between human injury and experimental SCI in rats will be important considerations.

Finally, while this study was performed with epidural electrodes over the motor cortex and spinal cord, SCAP might be applied with non-invasive stimulation. Part of the need for these rodent studies is to be able to manipulate specific neural circuits so that we know which ones need to be targeted. Should electrodes be needed for specific and effective recruitment, these methods are routinely used in clinical practice for other indications. As non-invasive stimulation techniques become better targeted, this may be a viable alternative, especially if the circuits that mediate this strong neuromodulation are clearly identified.

References:

Allred RP, Adkins DL, Woodlee MT, Husbands LC, Maldonado MA, Kane JR, Schallert T, Jones TA (2008) The vermicelli handling test: a simple quantitative measure of dexterous forepaw function in rats. J Neurosci Methods 170:229–244.

Anderson KD (2004) Targeting recovery: priorities of the spinal cord-injured population. J Neurotrauma 21:1371–1383.

Asboth L, Friedli L, Beauparlant J, Martinez-Gonzalez C, Anil S, Rey E, Baud L, Pidpruzhnykova G, Anderson MA, Shkorbatova P, Batti L, Pagès S, Kreider J, Schneider BL, Barraud Q, Courtine G (2018) Cortico-reticulo-spinal circuit reorganization enables functional recovery after severe spinal cord contusion. Nat Neurosci 21:576–588.

Baker SN, Perez MA (2017) Reticulospinal Contributions to Gross Hand Function after Human Spinal Cord Injury. J Neurosci 37:9778–9784.

Bastmeyer M, O'Leary DD (1996) Dynamics of target recognition by interstitial axon branching along developing cortical axons. J Neurosci 16:1450–1459.

Brus-Ramer M, Carmel JB, Martin JH (2009) Motor cortex bilateral motor representation depends on subcortical and interhemispheric interactions. J Neurosci 29:6196–6206.

Bunday KL, Perez MA (2012) Motor recovery after spinal cord injury enhanced by strengthening corticospinal synaptic transmission. Curr Biol 22:2355–2361.

Bunday KL, Urbin MA, Perez MA (2018) Potentiating paired corticospinal-motoneuronal plasticity after spinal cord injury. Brain Stimulat 11:1083–1092.

Bunge RP, Puckett WR, Becerra JL, Marcillo A, Quencer RM (1993) Observations on the pathology of human spinal cord injury. A review and classification of 22 new cases with details from a case of chronic cord

compression with extensive focal demyelination. Adv Neurol 59:75–89.

Capogrosso M et al. (2016) A brain-spine interface alleviating gait deficits after spinal cord injury in primates. Nature 539:284–288.

Carmel JB, Berrol LJ, Brus-Ramer M, Martin JH (2010) Chronic electrical stimulation of the intact corticospinal system after unilateral injury restores skilled locomotor control and promotes spinal axon outgrowth. J Neurosci 30:10918–10926.

Chandrasekaran S, Nanivadekar AC, McKernan G, Helm ER, Boninger ML, Collinger JL, Gaunt RA, Fisher LE (2020) Sensory restoration by epidural stimulation of the lateral spinal cord in upper-limb amputees. elife 9.

Engmann AK, Bizzozzero F, Schneider MP, Pfyffer D, Imobersteg S, Schneider R, Hofer A-S, Wieckhorst M, Schwab ME (2020) The Gigantocellular Reticular Nucleus Plays a Significant Role in Locomotor Recovery after Incomplete Spinal Cord Injury. J Neurosci 40:8292–8305.

Fitzgerald PB (2020) An update on the clinical use of repetitive transcranial magnetic stimulation in the treatment of depression. J Affect Disord 276:90–103.

Garcia-Sandoval A, Pal A, Mishra AM, Sherman S, Parikh AR, Joshi-Imre A, Arreaga-Salas D, Gutierrez-Heredia G, Duran-Martinez AC, Nathan J, Hosseini SM, Carmel JB, Voit W (2018) Chronic softening spinal cord stimulation arrays. J Neural Eng 15:045002.

Gerasimenko YP, Lavrov IA, Courtine G, Ichiyama RM, Dy CJ, Zhong H, Roy RR, Edgerton VR (2006) Spinal cord reflexes induced by epidural spinal cord stimulation in normal awake rats. J Neurosci Methods 157:253–263.

Giuffrida R, Rustioni A (1992) Dorsal root ganglion neurons projecting to the dorsal column nuclei of rats. J Comp Neurol 316:206–220.

Gu Z, Ueno M, Klinefelter K, Mamidi M, Yagi T, Yoshida Y (2019) Skilled movements in mice require inhibition of corticospinal axon collateral formation in the spinal cord by semaphorin signaling. J Neurosci 39:8885–8899.

Harel NY, Carmel JB (2016) Paired stimulation to promote lasting augmentation of corticospinal circuits. Neural Plast 2016:7043767.

Ichikawa H, Deguchi T, Nakago T, Jacobowitz DM, Sugimoto T (1994) Parvalbumin, calretinin and carbonic anhydrase in the trigeminal and spinal primary neurons of the rat. Brain Res 655:241–245.

Irvine K-A, Ferguson AR, Mitchell KD, Beattie SB, Beattie MS, Bresnahan JC (2010) A novel method for assessing proximal and distal forelimb function in the rat: the Irvine, Beatties and Bresnahan (IBB) forelimb scale. J Vis Exp.

Irvine K-A, Ferguson AR, Mitchell KD, Beattie SB, Lin A, Stuck ED, Huie JR, Nielson JL, Talbott JF, Inoue T, Beattie MS, Bresnahan JC (2014) The irvine, beatties, and bresnahan (IBB) forelimb recovery scale: an assessment of reliability and validity. Front Neurol 5:116.

Jo HJ, Perez MA (2020) Corticospinal-motor neuronal plasticity promotes exercise-mediated recovery in humans with spinal cord injury. Brain.

Kakulas BA, Kaelan C (2015) The neuropathological foundations for the restorative neurology of spinal cord injury. Clin Neurol Neurosurg 129 Suppl 1:S1-7.

Kathe C, Hutson TH, McMahon SB, Moon LDF (2016) Intramuscular Neurotrophin-3 normalizes low threshold spinal reflexes, reduces spasms and improves mobility after bilateral corticospinal tract injury in rats. elife 5.

Krashes MJ, Koda S, Ye C, Rogan SC, Adams AC, Cusher DS, Maratos-Flier E, Roth BL, Lowell BB (2011) Rapid, reversible activation of AgRP neurons drives feeding behavior in mice. J Clin Invest 121:1424–

1428.

Ling YT, Alam M, Zheng Y-P (2020) Spinal Cord Injury: Lessons about Neuroplasticity from Paired Associative Stimulation. Neuroscientist 26:266–277.

Madisen L et al. (2015) Transgenic mice for intersectional targeting of neural sensors and effectors with high specificity and performance. Neuron 85:942–958.

Mekhael W, Begum S, Samaddar S, Hassan M, Toruno P, Ahmed M, Gorin A, Maisano M, Ayad M, Ahmed Z (2019) Repeated anodal trans-spinal direct current stimulation results in long-term reduction of spasticity in mice with spinal cord injury. J Physiol (Lond) 597:2201–2223.

Mishra AM, Pal A, Gupta D, Carmel JB (2017) Paired motor cortex and cervical epidural electrical stimulation timed to converge in the spinal cord promotes lasting increases in motor responses. J Physiol (Lond) 595:6953–6968.

Moritz CT (2018) Now is the critical time for engineered neuroplasticity. Neurotherapeutics 15:628–634.

National Spinal Cord Injury Statistical Center, Facts and Figures at a Glance. Birmingham, AL: University of Alabama at Birmingham, 2020.

Nishimura Y, Perlmutter SI, Eaton RW, Fetz EE (2013a) Spike-timing-dependent plasticity in primate corticospinal connections induced during free behavior. Neuron 80:1301–1309.

Nishimura Y, Perlmutter SI, Fetz EE (2013b) Restoration of upper limb movement via artificial corticospinal and musculospinal connections in a monkey with spinal cord injury. Front Neural Circuits 7:57.

Park HG, Carmel JB (2016) Selective manipulation of neural circuits. Neurotherapeutics 13:311–324.

Porter R, Lemon R (1995) Corticospinal function and voluntary movement. Oxford University Press.

Raineteau O, Fouad K, Noth P, Thallmair M, Schwab ME (2001) Functional switch between motor tracts in the

presence of the mAb IN-1 in the adult rat. Proc Natl Acad Sci USA 98:6929–6934.

Ratnadurai Giridharan S, Gupta D, Pal A, Mishra AM, Hill NJ, Carmel JB (2019) Motometrics: A toolbox for annotation and efficient analysis of motor evoked potentials. Front Neuroinformatics 13:8.

Sangari S, Lundell H, Kirshblum S, Perez MA (2019) Residual descending motor pathways influence spasticity after spinal cord injury. Ann Neurol 86:28–41.

Sotocinal SG, Sorge RE, Zaloum A, Tuttle AH, Martin LJ, Wieskopf JS, Mapplebeck JCS, Wei P, Zhan S, Zhang S, McDougall JJ, King OD, Mogil JS (2011) The Rat Grimace Scale: a partially automated method for quantifying pain in the laboratory rat via facial expressions. Mol Pain 7:55.

Starkey ML, Bleul C, Zörner B, Lindau NT, Mueggler T, Rudin M, Schwab ME (2012) Back seat driving: hindlimb corticospinal neurons assume forelimb control following ischaemic stroke. Brain 135:3265–3281.

Stefan K, Kunesch E, Cohen LG, Benecke R, Classen J (2000) Induction of plasticity in the human motor cortex by paired associative stimulation. Brain 123 Pt 3:572–584.

Suppa A, Quartarone A, Siebner H, Chen R, Di Lazzaro V, Del Giudice P, Paulus W, Rothwell JC, Ziemann U, Classen J (2017) The associative brain at work: Evidence from paired associative stimulation studies in humans. Clin Neurophysiol 128:2140–2164.

Takeoka A, Vollenweider I, Courtine G, Arber S (2014) Muscle spindle feedback directs locomotor recovery and circuit reorganization after spinal cord injury. Cell 159:1626–1639.

Tan AM, Chakrabarty S, Kimura H, Martin JH (2012) Selective corticospinal tract injury in the rat induces primary afferent fiber sprouting in the spinal cord and hyperreflexia. J Neurosci 32:12896–12908.

Taylor JL, Martin PG (2009) Voluntary motor output is altered by spike-timing-dependent changes in the human corticospinal pathway. J Neurosci 29:11708–11716.

Vulchanova L, Schuster DJ, Belur LR, Riedl MS, Podetz-Pedersen KM, Kitto KF, Wilcox GL, McIvor RS, Fairbanks CA (2010) Differential adeno-associated virus mediated gene transfer to sensory neurons following intrathecal delivery by direct lumbar puncture. Mol Pain 6:31.

Wahl AS, Omlor W, Rubio JC, Chen JL, Zheng H, Schröter A, Gullo M, Weinmann O, Kobayashi K, Helmchen F, Ommer B, Schwab ME (2014) Neuronal repair. Asynchronous therapy restores motor control by rewiring of the rat corticospinal tract after stroke. Science 344:1250–1255.

Walters MC, Sonner MJ, Myers JH, Ladle DR (2019) Calcium imaging of parvalbumin neurons in the dorsal root ganglia. Eneuro 6.

Wen T-C, Lall S, Pagnotta C, Markward J, Gupta D, Ratnadurai-Giridharan S, Bucci J, Greenwald L, Klugman M, Hill NJ, Carmel JB (2018) Plasticity in one hemisphere, control from two: adaptation in descending motor pathways after unilateral corticospinal injury in neonatal rats. Front Neural Circuits 12:28.

Wolpaw JR (2018) The negotiated equilibrium model of spinal cord function. J Physiol (Lond) 596:3469–3491.

Yang Q, Ramamurthy A, Lall S, Santos J, Ratnadurai-Giridharan S, Lopane M, Zareen N, Alexander H, Ryan D, Martin JH, Carmel JB (2019) Independent replication of motor cortex and cervical spinal cord electrical stimulation to promote forelimb motor function after spinal cord injury in rats. Exp Neurol 320:112962.

Figure Legends:

Figure 1. The immediate effects of pairing depend on timing. **A.** Schematic of paired stimulation. **B.** Experimental paradigm of immediate effect testing. Supra-threshold (110% of cortical threshold) stimulation of the motor cortex produces an MEP that is modulated by subthreshold (90% of spinal threshold) spinal cord stimulation. **C.** Immediate effects of paired stimulation depend on latency. We tested different latencies between motor cortex and spinal cord stimulation from −30 ms to 30 ms. As indicated by the insets, negative times indicate that spinal cord was stimulated before motor cortex stimulation and positive times indicate that spinal cord was stimulated after motor cortex stimulation. Maximum augmentation was found when spinal cord stimulation was delivered 9ms, 10 ms and 11ms after motor cortex stimulation (peak at 10ms). MEPs were significantly elevated at the time points indicated, as measured by t-test with Bonferroni correction compared to no spinal stimulation baseline * = $p < 0.05$ ($n = 4$).

Figure 2. CST inactivation abrogates paired stimulation. A. Paradigm AAV1-hSyn-DIO-hM4D(Gi)-mCherry was injected into the forelimb area of the primary motor cortex and AAV2/retro-pmSyn1-EBFP-Cre was injected into the right side of the C5 & C6 spinal segments. **B**. Dual virus transduction drives robust mCherry expression in corticospinal neurons located in motor cortex layer 5 (dotted lines). **C.** CST inactivation impairs skilled forepaw use. The number of adjustments of both forepaws was counted while the animal was eating uncooked pasta before and at 30, 60, and 120 minutes after clozapine N-oxide (CNO) injection. Inactivation significantly reduces the paw manipulations in the inactivated paw. **D.** CST inactivation abrogates the effect of paired stimulation. One week after the behavioral test, the CST was inactivated by CNO injection. The augmentation of

paired stimulation was fully abrogated at 20-60 minutes in the inactivation side and gradually recovered (n=3).

Figure 3. Afferent inactivation abrogates paired stimulation. A. An AAV5 encoding the inactivating DREADD was injected into DRG on one site as the targeted side. **B.** DREADD in neurons (arrow head), infected with the virus measured 67.9±18.5μm in diameter, similar to neurons that mediate touch, proprioception, and muscle length/tension. **C.** Inactivation abrogates paired stimulation in rats infected with AAV5-DREADD, targeted side (red line) compared to non-targeted side (grey line) (n=2), 100% suppression at 40 minutes after CNO injection. **D.** A Cre-dependent DREADD was injected into the DRG on the inactivation side of rats expressing Cre under control of parvalbumin, which is expressed selectively by proprioceptors. **E.** DREADD in proprioceptive neurons (arrow head), infected with the virus. **F.** Inactivation abrogates paired stimulation in PV-Cre rats, inactivation side (green line) compared to baseline (n=3); more than 70% suppression of paired stimulation effect at 40 minutes after CNO injection. More selective inactivation (green line) resulted in 25.8% ± 3.8% suppression of sensory afferents while non-selective (red line; -1.5% ±10.5%) inactivation caused more robust suppression of paired stimulation responses on the targeted side of forelimb after CNO injection. Vehicle (normal saline) injection did not change MEPs compared to baseline both on the targeted side (df=2, Cohen's d=0.574, p=0.624) or the non-targeted side (df=2, Cohen's d=1.11, p=0.383, data not shown).

Figure 4. SCAP Protocol Optimization. A. Effect second stimulation over the first stimulation for different frequencies. **B**. Protocol to test the effects of different numbers of pair pulse train, time intervals between the pulse train and repeated trains. **C.** Effects of

number of stimuli in a train (150 stimuli are optimum), time interval between trains (1 min was as good as 5 min) and number of trains (10x and 20x are similar) on average MEPs over the 120 minutes of testing.

Figure 5. Spinal Cord Associative Plasticity (SCAP) Protocol: A. Baseline measurements of cortical MEP, spinal MEPs and thresholds before repetitive pairing. Cortical and spinal stimulation at 110% of the cortical and spinal thresholds. MEPs recorded from the biceps. Threshold was determined by adjusting stimulation intensity to provoking a short-latency EMG in >50% of trials. **B.** Repetitive paired stimulation, repetitive pairing motor cortex and spinal cord stimulation at 10 ms latency for 30 minutes. **C.** Testing the effects of 30 Minutes SCAP, cortical, spinal MEPs and thresholds were measured as it was done before SCAP. **B1.** 5 minute SCAP protocol. **B2.** A 30-minutes SCAP paradigm (5 Hz, 150 pairs of cortical and spinal stimuli 20 times with 1 minute gap between bursts, delivering a total of 3000 pairs).

Figure 6. SCAP causes lasting changes in cortical and spinal cord excitability in uninjured rats and rats with SCI. A. Cortical and spinal MEP augmentation after 30min SCAP in uninjured awake rats (n=4) is comparable to 5min SCAP in uninjured awake rats (n=6). **B.** Cortical and spinal excitability. **C.** Cortical and Spinal MEPs in rats with C4 SCI. 5min SCAP (n=2) was compared with 30min SCAP (n=5). **D.** Cortical and Spinal Excitability in SCI rats. In both injured and uninjured groups of rats after 30minutes of repetitive pairing both cortical and spinal evoked responses were augmented for more than 2 hrs and this augmentation persisted even after SCI, similarly the excitability increased till 2 hrs after pairing. Excitability = 1/ threshold. **E.** Average MEP augmentation over 120

minutes with different SCAP conditions. Pairing at an inappropriate latency (100ms), only motor cortex or only spinal cord stimulation do not result in elevated MEP responses.

Figure 7. Experimental timeline. Rats were trained on the food manipulation task and then subjected to C4 contusion injury. Rats were randomized to SCAP daily for 10 days (stimulation group) versus sham (no) stimulation (control group). Physiology and behavior testing was done before stimulation on and then weekly after stimulation. Rats were sacrificed and lesion volume was measured at the end of the trial.

Figure 8. Ten days of SCAP produces augmented MEPs for at least 50 days after SCI. The immediate effects were not different before stimulation (day 11), and increased in the rats with stimulation (n=5) but not in controls (n=4).

Figure 9. Reduced hyperreflexia with SCAP. A. Method of H-reflex testing. **B.** The second H-reflex is diminished (arrow) at short inter-stimulus intervals. **C.** Rats with stimulation (n=5). Less H-reflex depression in rats 5 days after SCI (dark red) compared to before (blue). After paired stimulation H-reflex depression was largely restored and maintained in the stimulation group. **D.** Control rats (n=4) do not show restoration of H-reflex modulation. M= M-wave, H= H-reflex.

Figure 10. SCAP promotes motor recovery after SCI and does not affect pain. A. Schematics showing characteristic features of rat forelimbs during cereal manipulation task. Images of a representative stimulation rat were generated from frames of live videos with the image tracing tool of Adobe Illustrator software. Score 9 at baseline before SCI: Volar (palm) support, paw adapts to the shape of the cereal. Score 5 after stimulation: Volar support, digit 2 contributes to cereal manipulation, other digits extended. Score 3 after

injury, before stimulation: Lack of volar support, extended digits, paw doesn't adapt to the shape of the cereal. **B.** Rats in the stimulation group (n=5) had higher dexterity scores than the control group (n=4) at 50 days after SCI (df =7, Cohen's d= 1.83, p=0.029). **C.** No increase in pain score with 10 days of repetitive stimulation, rats in both the groups did not experience pain during the stimulation phase (p=0.51).

Figure. 11. Stimulation and control animals received similar injuries. A. Force applied during cervical contusion (n=5 for stimulation, n=4 for control rats). **B**. Representative spinal cord sections showing the extent of the lesion, scale bar: 1 mm. **C.** Spared tissue area through the lesioned spinal cord.

Figures:

Figure 1:

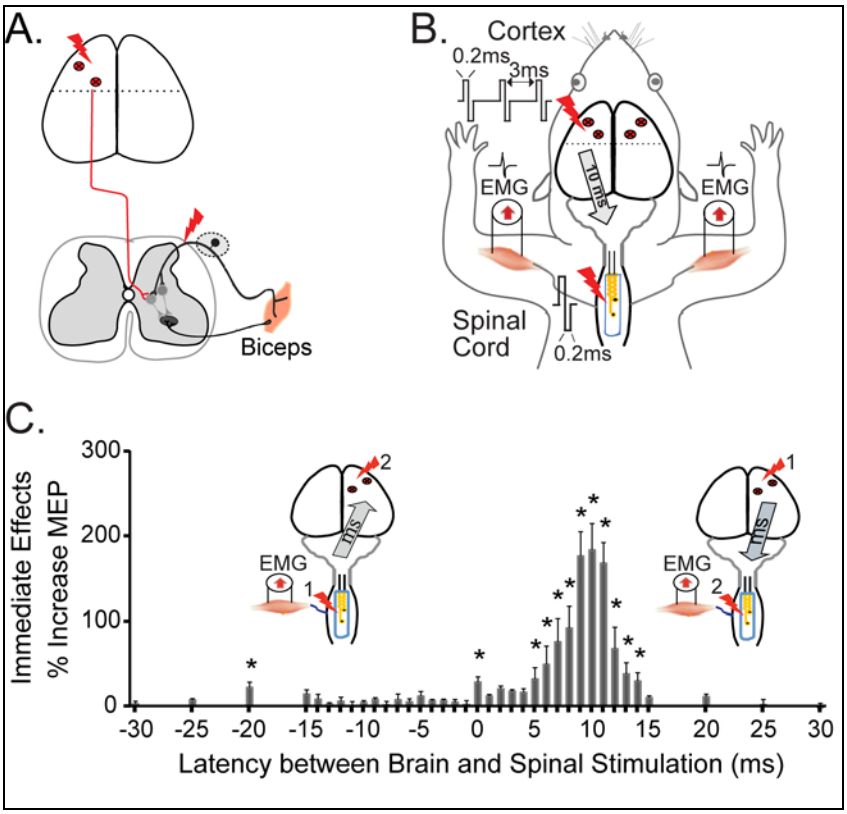

Figure 2:

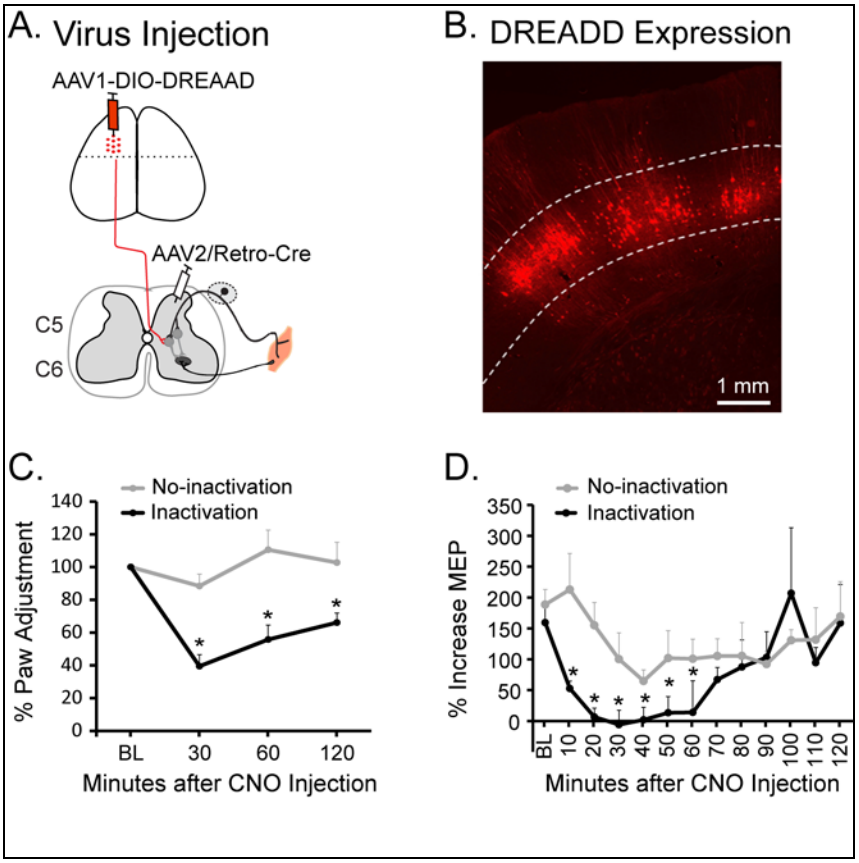
A. Virus Injection
AAV1-DIO-DREAAD
AAV2/Retro-Cre
C5
C6
B. DREADD Expression
1 mm
C.
No-inactivation
Inactivation
% Paw Adjustment
140
120
100
80
60
40
20
0
BL
30
60
120
Minutes after CNO Injection
D.
No-inactivation
Inactivation
% Increase MEP
350
300
250
200
150
100
50
0
BL
10
20
30
40
50
60
70
80
90
100
110
120
Minutes after CNO Injection

Figure 3:

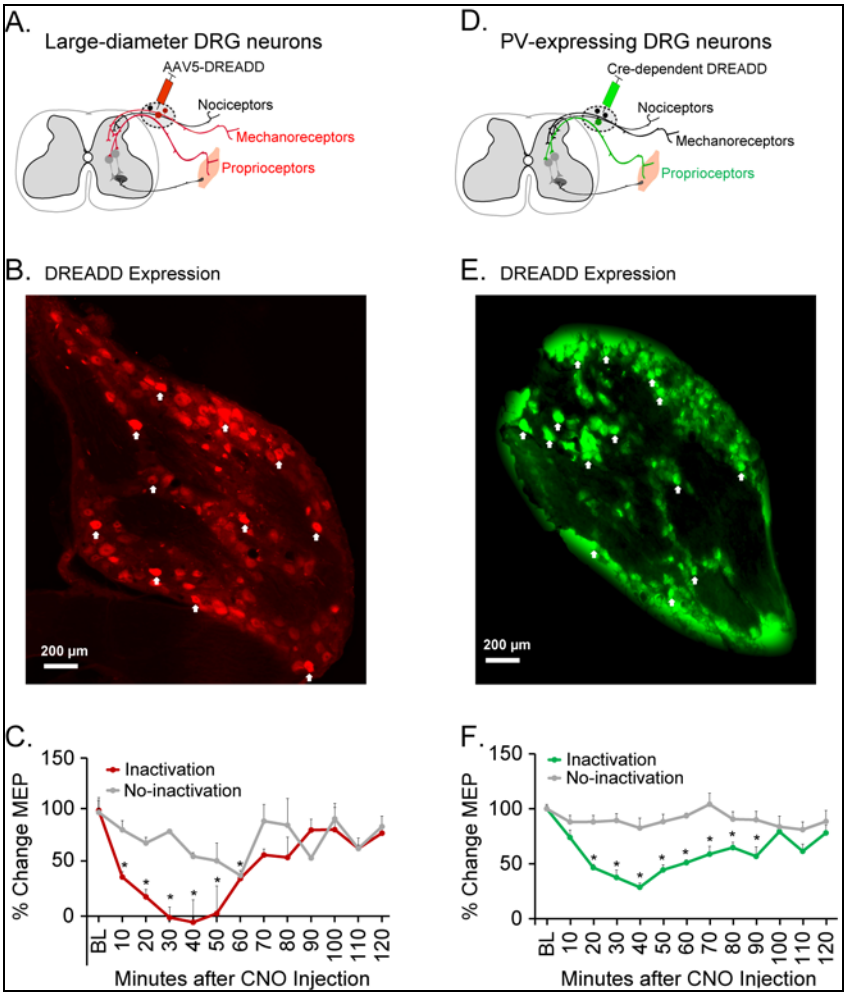
A.
Large-diameter DRG neurons
AAV5-DREADD
Nociceptors
Mechanoreceptors
Proprioceptors
D.
PV-expressing DRG neurons
Cre-dependent DREADD
Nociceptors
Mechanoreceptors
Proprioceptors
B. DREADD Expression
200 µm
E. DREADD Expression
200 µm
C.
% Change MEP
Inactivation
No-inactivation
Minutes after CNO Injection
F.
% Change MEP
Inactivation
No-inactivation
Minutes after CNO Injection

Figure 4:

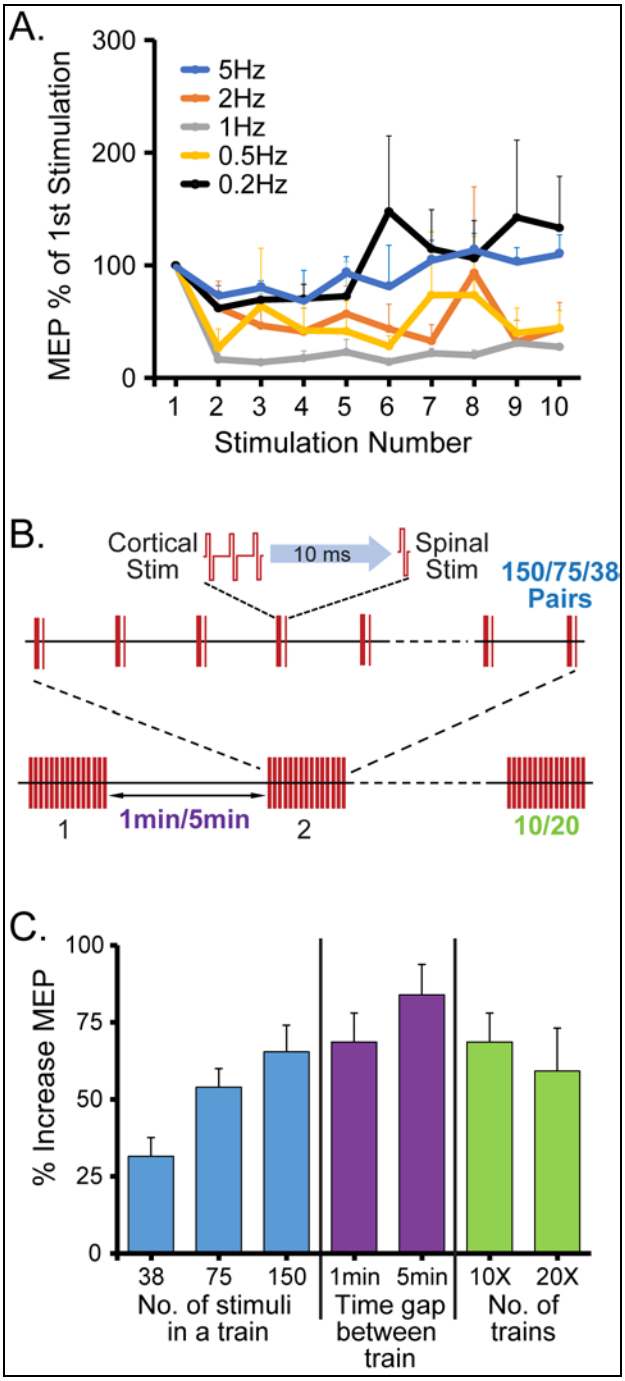
A.
MEP % of 1st Stimulation
300
200
100
0
5Hz
2Hz
1Hz
0.5Hz
0.2Hz
1 2 3 4 5 6 7 8 9 10
Stimulation Number
B.
Cortical Stim
10 ms
Spinal Stim
150/75/38 Pairs
1
1min/5min
2
10/20
C.
% Increase MEP
100
75
50
25
0
38 75 150
No. of stimuli in a train
1min 5min
Time gap between train
10X 20X
No. of trains

Figure 5:

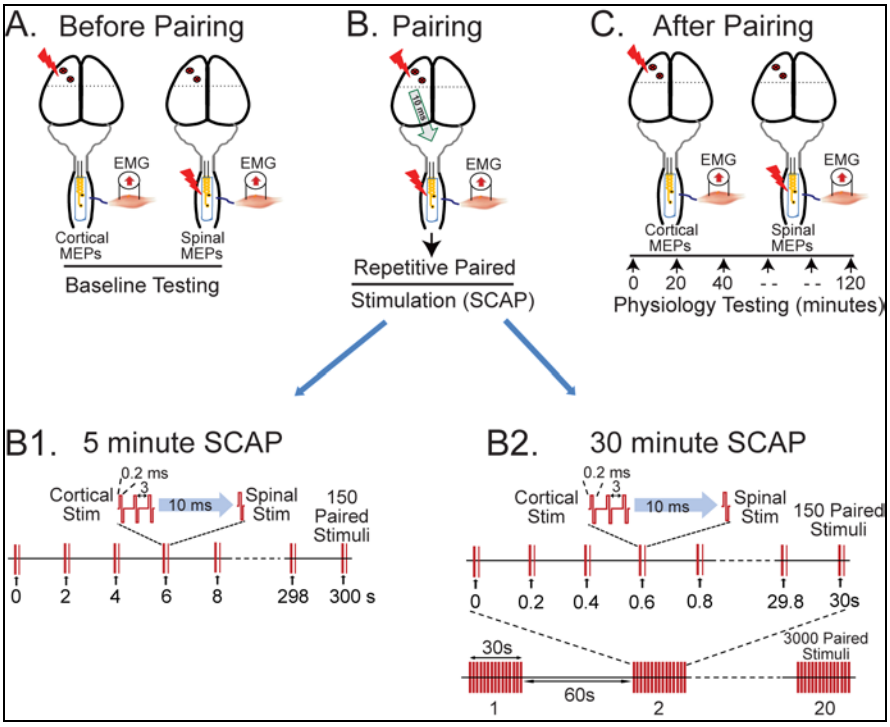
A. Before Pairing
EMG
EMG
Cortical MEPs
Spinal MEPs
Baseline Testing
B. Pairing
10 ms
EMG
Repetitive Paired Stimulation (SCAP)
C. After Pairing
EMG
EMG
Cortical MEPs
Spinal MEPs
0 20 40 - - - - 120
Physiology Testing (minutes)
B1. 5 minute SCAP
0.2 ms
3
Cortical Stim
10 ms
Spinal Stim
150 Paired Stimuli
0 2 4 6 8 298 300 s
B2. 30 minute SCAP
0.2 ms
3
Cortical Stim
10 ms
Spinal Stim
150 Paired Stimuli
0 0.2 0.4 0.6 0.8 29.8 30s
30s
60s
3000 Paired Stimuli
1 2 20

Figure 6:

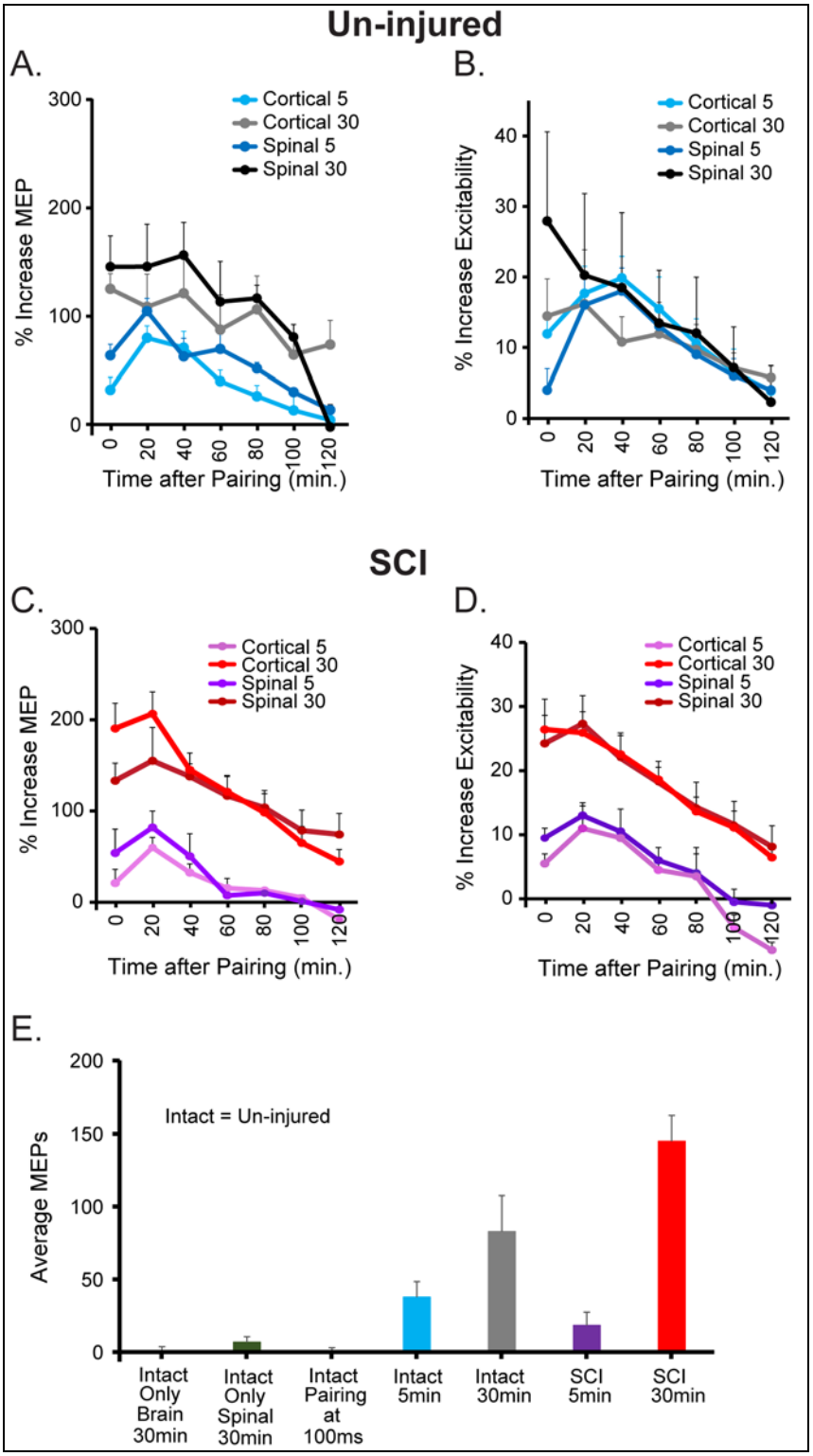
Un-injured
A.
B.
Cortical 5
Cortical 30
Spinal 5
Spinal 30
% Increase MEP
% Increase Excitability
Time after Pairing (min.)
SCI
C.
D.
E.
Intact = Un-injured
Average MEPs
Intact Only Brain 30min
Intact Only Spinal 30min
Intact Pairing at 100ms
Intact 5min
Intact 30min
SCI 5min
SCI 30min

Figure 7:

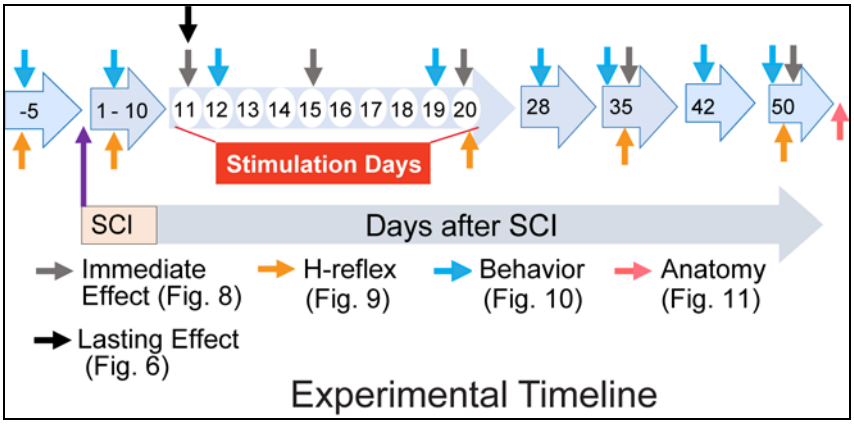

Figure 8:

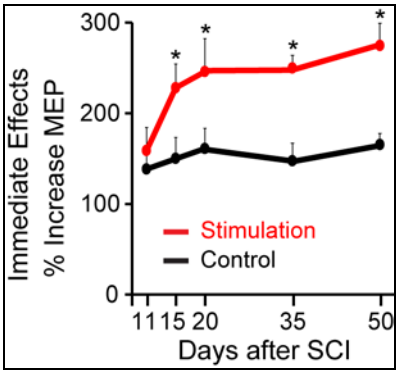

Figure 9:

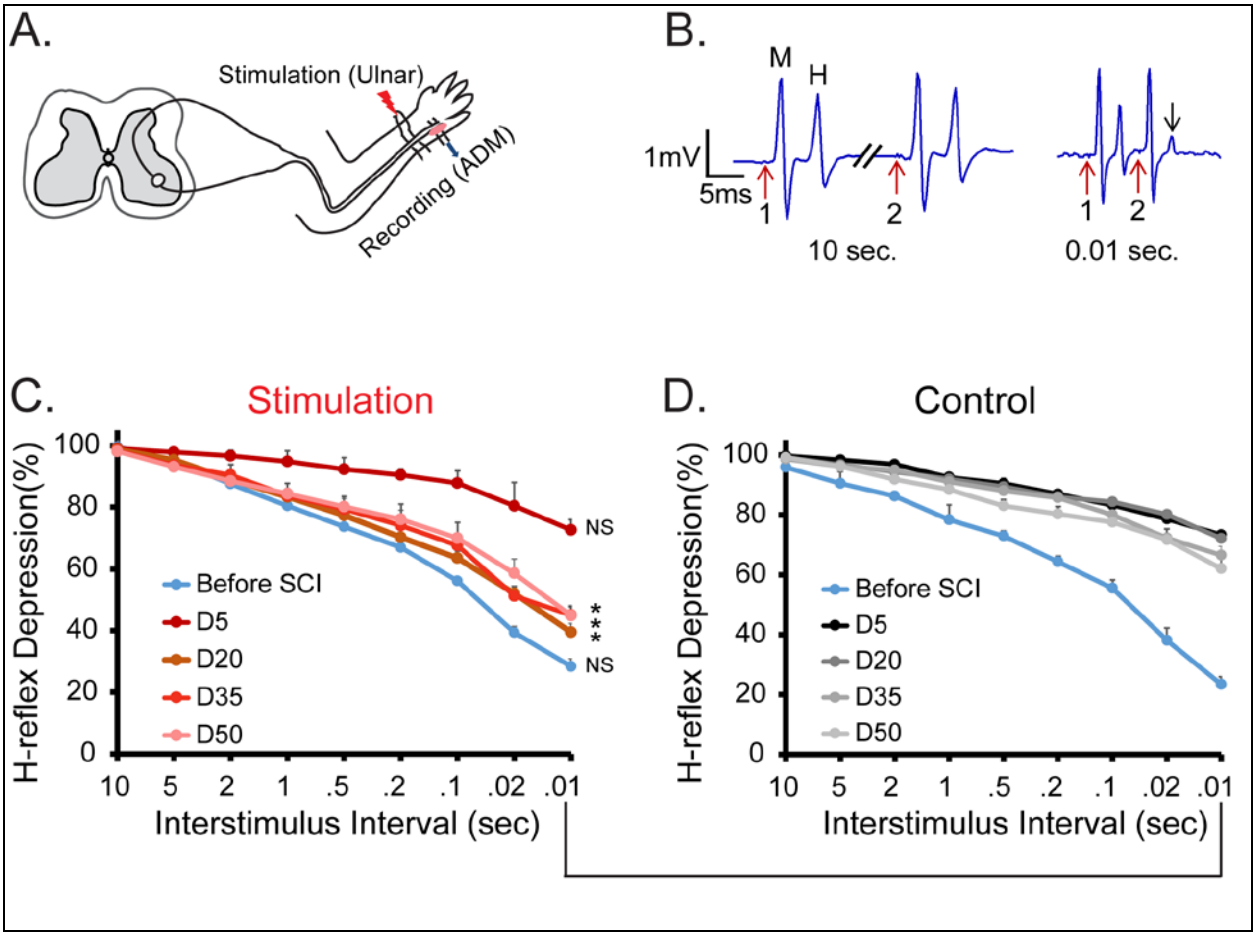
A.
Stimulation (Ulnar)
Recording (ADM)
B.
M
H
1mV
5ms
1
2
10 sec.
1
2
0.01 sec.
C.
Stimulation
H-reflex Depression(%)
100
80
60
40
20
0
Before SCI
D5
D20
D35
D50
NS
***
NS
10 5 2 1 .5 .2 .1 .02 .01
Interstimulus Interval (sec)
D.
Control
H-reflex Depression(%)
100
80
60
40
20
0
Before SCI
D5
D20
D35
D50
10 5 2 1 .5 .2 .1 .02 .01
Interstimulus Interval (sec)

Figure 10:

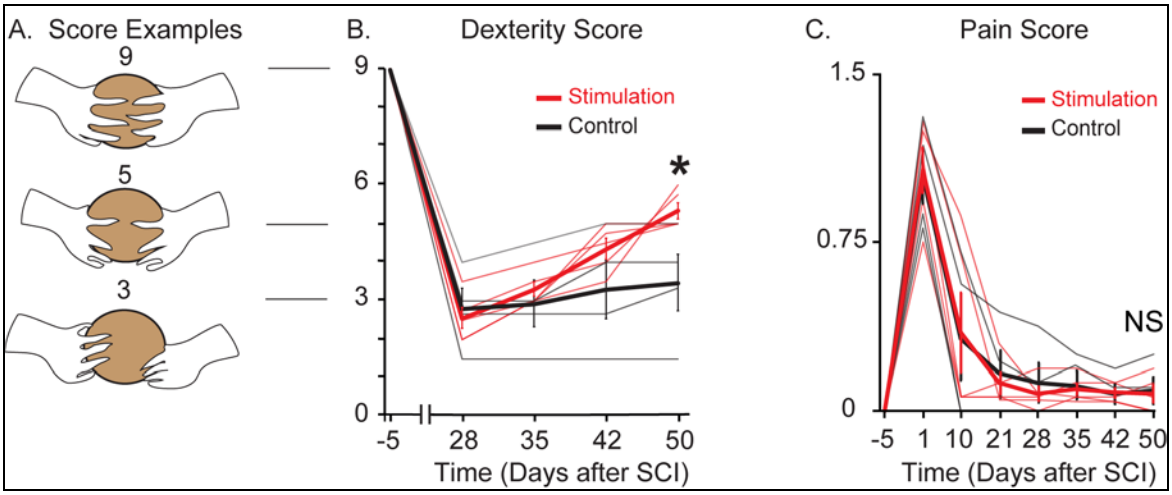
A. Score Examples
9
5
3
B. Dexterity Score
Stimulation
Control
*
9
6
3
0
-5
28
35
42
50
Time (Days after SCI)
C. Pain Score
Stimulation
Control
NS
1.5
0.75
0
-5
1
10
21
28
35
42
50
Time (Days after SCI)

Figure 11:

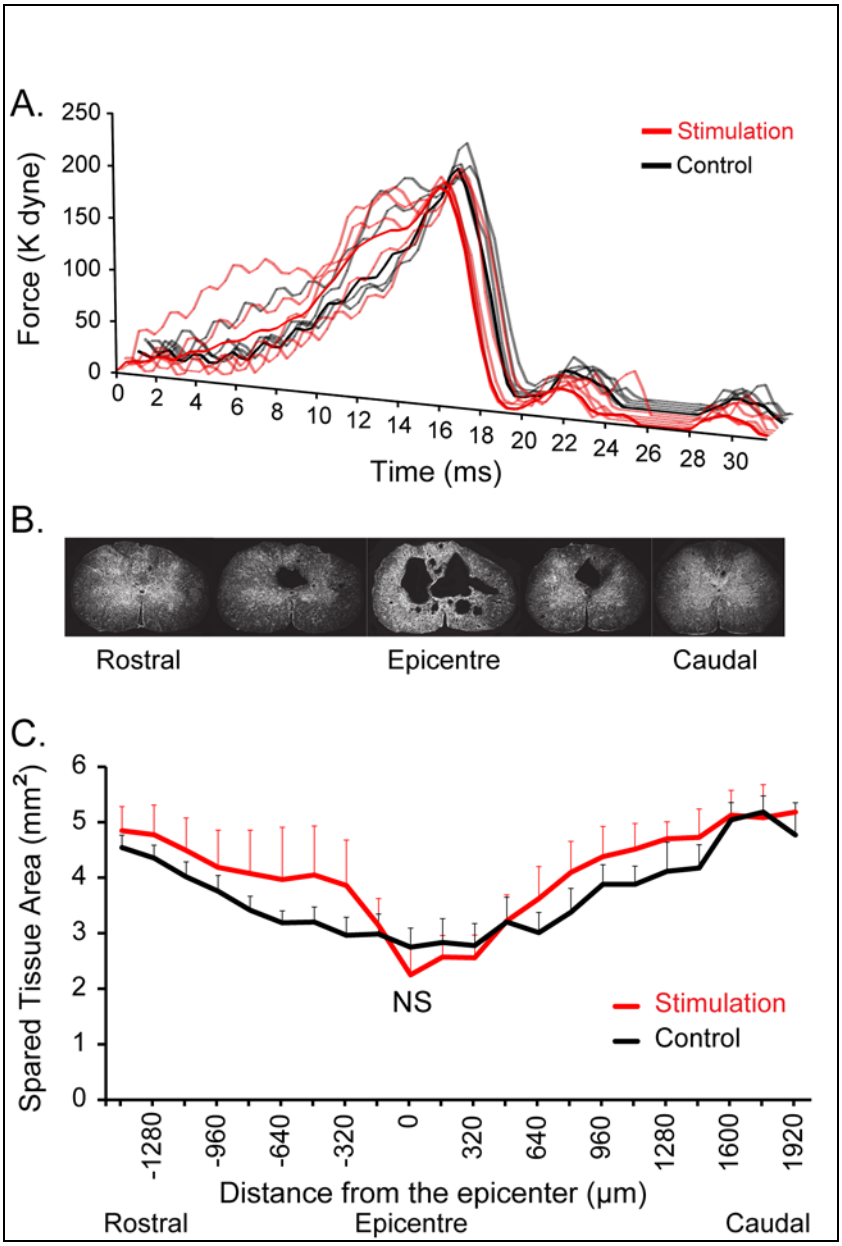
A.
Force (K dyne)
250
200
150
100
50
0
0 2 4 6 8 10 12 14 16 18 20 22 24 26 28 30
Time (ms)
Stimulation
Control
B.
Rostral
Epicentre
Caudal
C.
Spared Tissue Area (mm²)
6
5
4
3
2
1
0
NS
Stimulation
Control
-1280 -960 -640 -320 0 320 640 960 1280 1600 1920
Distance from the epicenter (µm)
Rostral
Epicentre
Caudal